Journal of Applied Polymer Science

Process Optimization of Electrospun Silk Fibroin Fiber Mat for Accelerated Wound Healing

Jesada Chutipakdeevong,[1] Uracha Rungsardthong Ruktanonchai,[2] Pitt Supaphol[1]

[1]The Petroleum and Petrochemical College, Chulalongkorn University, Pathumwan, Bangkok 10330, Thailand

[2]National Nanotechnology Center, National Science and Technology Development Agency (NSTDA), Thailand Science Park, Klong Luang, Pathumthani 12120, Thailand

Correspondence to: U. R. Ruktanonchai (E-mail: uracha@nanotec.or.th) or P. Supaphol (E-mail: pitt.s@chula.ac.th)

ABSTRACT: Considering the outstanding biocompatibility of *Bombyx mori* silk fibroin, this study is designed to fabricate biomimetic nanofibrous structure made of silk fibroin, which can enhance cell activities for tissue formation. The electrospinning of blend of silk fibroin with low molecular weight poly(ethylene-oxide) (PEO) is explored with ease of preparation for high productivities. The average diameter of electrospun silk fibroin (eSF) is decreased from 414 ± 73 to 290 ± 46 nm after PEO extraction. To induce the desired cellular activity, the surface of the eSF fibers is modified with fibronectin by using the carbodiimide chemistry method. The potential use of the obtained wound healing material is assessed by indirect cytotoxicity evaluation on normal human dermal fibroblast (NHDF) in terms of their attachment and cell proliferation. The surface-modified eSF nanofiber mats show good support for cellular adhesion and spreading as a result of fibronectin grafting on the fiber surface, especially for cell migration inside the fibrous structure. These results demonstrate a new fabrication technique of surface-modified silk fibroin electrospun nanofibers for biomedical application; with the ability to accelerate wound healing. © 2013 Wiley Periodicals, Inc. J. Appl. Polym. Sci. 130: 3634–3644, 2013

KEYWORDS: biomedical applications; biopolymers & renewable polymers; biomaterials

Received 26 February 2013; accepted 3 June 2013; Published online 26 June 2013

DOI: 10.1002/app.39611

INTRODUCTION

Nowadays, there are numerous researches regarding the relative efficiency of the various kinds of material for effective wound healing. Biopolymers and fabrication techniques have been studied not only for closing and covering wounds in order to prevent infection but also have extraordinary properties that promote the healing process [1–3] Generally, the wound healing process can be divided into three phases: inflammation, proliferation, and tissue remodeling.[1] The healing process is a complicated system that involves the interaction of many types of cells. Fibroblasts are one of the most abundant cell types in connective tissues that become activated and can differentiate into myofibroblasts when tissues are injured.[4] The ideal candidate for promotion of wound healing should mimic the structure and biological environment of the wounds, i.e., native extracellular matrix (ECM) proteins, which provide support and biological functions for cellular activities.[5] To meet such specification, it is necessary to choose the appropriate biomaterial for the fabrication of nanofibrous scaffold for tissue engineering.

Domesticated, *Bombyx mori*, silkworms are widely available in Thailand, which is well known in the textile industry for centuries. Silk fibroin (SF) from the silk cocoon is generally defined as an attractive biomaterial because of its unique characteristics such as high mechanical strength, excellent biocompatibility, controllable structure and morphology, and wide variety of constructive properties on tissue engineering.[6–9] The fibroin fibers are composed of three proteins: a heavy chain (~350 kDa), a light chain (~25 kDa), and small glycolprotein (~30 kDa).[8] The light chain fibroin exhibits the best properties—higher hydrophilicity, water uptake ability, low degradation rate, and superior cell adhesion properties. This may then introduce its potential uses as has been previously reported (e.g., films, foams, hydrogels, sphere, and fibers)[8–10] The amino acid composition of SF from *B. mori* consists primarily of glycine (43%), alanine (30%), and serine (12%), which is composed of repeated motifs, $[GAGSGA]_n$ in the crystalline domain.[9,11,12] In addition, major interest of SF for wound dressing application is due to the fact that silk can be engineered to degrade at slow rate because of its high crystallinity induced by β-sheet structure formation. Therefore, the slow degradation of silk mats will

not cause any inflammatory reaction and interference with healing process.[20]

Biomaterial-scaffold design is an important element for tissue engineering. Electrospinning is of interest in this study as it can produce nonwoven nanofibers mat with a unique three-dimensional structure that mimics the topographic features and biological function of collagen structure in natural ECM.[5] The important advantages of electrospinning technique are that it can generate loose porous fibrous membrane with high porosity and surface area, which can be an excellent candidate for many biomedical applications ranging from drug delivery, tissue engineering, implants, and wound dressing. Numerous researches of SF electrospun were focused on the preparation of electrospinning solution that was usually prepared in formic acid to produce cylindrical or ribbon like fibers where they demonstrated good biocompatibility with a variety of cell.[6,16,18,21,26] Electrospun SF (eSF) can be produced in a wide range of diameters from a few nanometers to micrometers depending on the process. The effect of silk solution viscosity, cause of solution concentration, was the most important factor on morphology and fibers diameter. From our previous report, eSF prepared by formic acid has the fiber diameters ranging between 210 and 670 nm.[18] Consequently, electrospinning of composite material based on SF were also studied such as poly(ethylene oxide) (PEO, 900 kDa), which was used as additive viscosity of aqueous SF solution, yielding the uniform electrospun fiber with significantly diameter ranging in submicron.[15,19,22,24,27,28] Almost all of PEO could be removed by subsequently washing the fiber with water after induction of β-sheet formation to reduce toxicity. Beyond that, introducing adsorption and chemical immobilization of protein, such as BMP-2, RGD, and fibronectin, has been explored as cellular binding sites for integrin receptors and impact cellular adhesion and proliferation.[9,19,22,28,29]

In this study, we aimed to optimize the preparation process for ultra-fine eSF fibers. Electrospinning from blends of Thai SF in aqueous solution were studied in order to achieve the effective ingredient for electrospinning. The concentration effects of low molecular weight PEO (600 kDa) and relative humidity on morphology were investigated prior to PEO extraction. The surface immobilization of fibronectin, which plays a major role in physiological process, on eSF was carried out by wet chemical method to improve cellular spreading. The potential for use of eSF fiber mats as wound dressing was evaluated by *in vitro* cellular respond using human fibroblasts, in which the attachment and proliferation activities were investigated.

EXPERIMENTAL

Materials

Fresh Thai silk cocoons of *B. mori* silkworms (Chul 1/1) were generously provided by Chul Thai Silk (Phetchabun, Thailand). Poly(ethylene oxide) (PEO, 600 kDa) was purchased from Acros organics (Geel, Belgium). One-ethyl-3-(dimethylaminoprophyl) carbodiimide hydrochloride (EDC), N-hydroxysuccinimide (NHS) and fibronectin were purchased from Sigma (Sigma, USA). The chemicals used for the preparation of eSF and its spinning solutions were sodium carbonate (Na_2CO_3), lithium bromide (LiBr), were purchased from Riedel-de Haën (Germany). Normal human dermal fibroblast (NHDF) cells were obtained from the American Type Culture Collection (ATCC, USA). Others chemicals used in cell study were purchased from Invitrogen (USA). All chemicals were of analytical grade and used without further purification.

Preparation of Electrospinning Solution

Thai *B. mori* silk cocoons were degummed by boiling in an aqueous solution of 0.02*M* Na_2CO_3 for 30 min three times, and then rinsed with warm distilled water to get rid of sericin proteins. SF was extracted from the degummed silk treads by dissolving in 9.3*M* LiBr (55°C) for 30 min at a final concentration of approximately 10% (w/v). The solution was dialyzed in distilled water using dialysis tubing cellulose membrane (Sigma-Aldrich, USA) for 3 days. The dialysate was centrifuged at 5°C for 20 min. The SF solution was filtered and lyophilized using LABCONCO: FreezeZone 6 to obtain the regenerated SF sponges. SF/PEO blend in aqueous solution was used for electrospinning. The SF sponges and PEO (600 kDa) was mixed at various weight ratios and stirred for 12 h at room temperature. The electrospinning solution was prepared at 10% (w/v) of SF/PEO blending concentration.

Preparation of eSF Nanofibers via Electrospinning

During electrospinning process, a homogeneous solution of SF/PEO was contained in a 20 mL glass syringe. A high electric potential in the range of 12–14 kV was applied to a droplet of the solution at a tip of a gauge 20 syringe needle. A jet of the SF solutions was ejected to a grounded rotating drum (rotation speed ~100 rpm) with aluminum foil attached. The distance between the tip of the needle and the drum was fixed at 15 cm. The syringe and the needle were tilted ~ 45° to maintain the flow rate of the electrospinning solution (flow rate ~1 mL/h) at the tip of the needle. The electrospun nanofibers were processed under the various relative humidity in the range from 30% to 60% at the ambient temperature. The suitable condition was chosen for electrospinning to obtain nanofiber mats.

Fibers Treatment and Surface Modification of eSF

The water soluble SF/PEO fiber mats were immersed in 98% methanol for 10 min and air dried to induce the conformation from amorphous (unstable silk I) to β-sheet transition (silk II), which was water-insoluble. Treated fiber mats were washed in distilled water at 37°C for 3 days to remove PEO. The PEO extracted SF fiber mats were put into a phosphate buffered saline (PBS) for 30 min to hydrate and stimulate the -COOH groups on aspartic and glutamic residues on the surface of eSF. Then the fibers were reacted with EDC/ NHS solution (0.5 mg/mL of EDC with 0.7 mg/mL of NHS in PBS buffer) for 15 min at room temperature to create activated functional group on the surface. The activated fiber mats were rinsed with PBS buffer, then treated with 0.1 mg/mL fibronectin in the PBS for 2 h at ambient temperature and rinsed with PBS three times followed by distilled water to get rid of excess peptide and salts before air-dried.[29,30]

Scanning Electron Microscopy

Hitachi S-4800 Ultra-high resolution cold Field Scanning Electron Microscope (FE-SEM) was used to observe morphology and size of the electrospun fibers by operating at 10 kV. The

samples were attached carefully on the stub, and then sputter coated with platinum before analysis. The fibers sizes were determined by measuring randomly from SEM images by using SemAphore 4.0 program

Fourier Transform Infrared Spectroscopy

All infrared spectra of electrospun fibers were recorded by using Thermo Nicolet Nexus 670 Spectrophotometer. Each spectrum was recorded by the accumulation of 32 scans with a resolution of 4 cm^{-1} in a range of 400 to 4000 cm^{-1}. The measurement was achieved by using ZnSe crystal cell with an attenuated total reflectance fourier transform infrared (ATR-FTIR) mode.

Water Retention and Dissolution Behavior

Neat eSF and surface modified eSF fiber mats were completely dried at 60°C for 24 h, prior to storage in the desiccators overnight to equilibrium to observe the initial dry weight (W_i) of the neat and surface-modified fiber specimens. At designed time points, both of electrospun fiber mats were immersed in PBS buffer at 37°C. The wet weight of the fiber mats (W_f) was determined after the elimination of excess water. The water content of the electrospun fiber mats were calculated as follows:

$$\text{Water content}\,(\%) = (W_f - W_i)/W_i \times 100$$

The fiber mats then were dried to a constant weight at 50°C for 24 h prior to storage in desiccator overnight. The final dry weight (W_d) after specified time of incubations was recorded to calculate to the percentages of remaining weight as follows:

$$\text{Mass remaining}\,(\%) = 100 - (W_i - W_d)/W_i \times 100$$

X-ray Photoelectron Spectroscopy

To study the grafting efficiency of the eSF, the analysis was carried out by using a Thermo Fisher Scientific Thetaprobe X-ray Photoelectron Spectroscopy (XPS), Singapore. Monochromatic Al Kα X-ray was employed for analysis of one spot on each sample with photoelectron take-off angle of 50° (with respect to surface plane). The analysis area was approximately 400 μm × 400 μm, whereas the maximum analysis depth lay in the range of ~4–8 nm. A special designed electron flood gun with a few eV Ar^+ ion was used for the charge compensation. Further correction was made based on adventitious C 1s at 285.0 eV using the manufacturer's standard software. Survey spectra were acquired for surface composition analysis with Scofield sensitivity factors.

Indirect Cytotoxicity Evaluation

Cytoxicity of the neat and surface-modified eSF with fibroin was evaluated by an indirect method, adapted from the ISO 10993-5 standard test method, by using NHDFs (NHDF, 15th passage). The cells were incubated in Dulbecco's modified Eagle's medium (DMEM) by adding a requisite amount of 10% fetal bovine serum (FBS), 1% l-glutamine, and 1% antibiotic and antimycotic formulation, which contained penicillin G sodium, streptomycin sulfate, and amphotericin B. For the cell culture, the specimens were sterilized by UV radiation for about 2 h. They were then immersed in a serum-free medium (SFM; DMEM containing 1% l-glutamine, 1% lactalbumin, and 1% antibiotic and antimycotic formulation) for 24 h at the extraction ration of 5, 10, and 20 mg/mL, and then the fiber mats were removed from the medium that were used later for cell culture study. The cells of NHDF were cultured separately in 24-well tissue-culture polystyrene plates (TCPS) at 10,000 cells/well in DMEM for 24 h. The medium was replaced with each of extraction medium and re-incubated for 24 h. The cell viability was assessed by using 3-(4,5-dimethylthiazol-2-yl)-2,5-diphenyltetrazolium bromide (MTT) assay, which is based on the basis of the reduction of the yellow tetrazolium salt to purple formazan crystals by active cells. First, according to the cell cultured method, the medium of cultured cells was removed and replaced with MTT solution directly on the fiber specimens and then the plate was incubated for 1 h. After incubation, the solution of DMSO was added to dissolve the formazan crystals. The number of the viable cells was observed by the amount of purple formazan crystals that was measured by SpectraMax M2 microplate reader. The absorbance value of the cell with fresh SFM was used as control (I_c), which is used as a reference to calculate % cell viability of each substrate, where the I_s is the absorbance value of cell of substrate.

$$\%\ \text{cell viability of substrate} = I_s/I_c \times 100$$

Cell Attachment and Proliferation Test

For the cell attachment study, both the neat and modified eSF fiber specimens (fiber mats of about 1.4 cm in diameter) were sterilized by UV radiation about 1 h for each side. The specimens were then placed in 24-well TCPS. The NHDFs cells were then cultured on the surface of both fiber mats and in glass slides (i.e., positive control) for 2, 4, and 8 h and then incubated in 5% CO_2 at 37°C. For the cell proliferation study, the cells, after having been allowed to attach on the substrates for 24 h, were cultured for 1, 2, and 3 days. After each cell-culturing time point, the viability of the attached and proliferated cells was determined by MTT assay.

Morphological Observation of Cultured Cells

The cell morphology changed with time on the eSF fiber mats was characterized by FE-SEM. After the culture medium had been removed, the cell-cultured fiber mats were rinsed twice with PBS and the cells were then fixed with 3% glutaraldehyde/PBS solution (Electron Microscopy Science, USA) for 30 min. After fixation of cells, the cell-cultured specimens were rinsed again with PBS, prior to being dehydrated at various concentrations of ethanol aqueous solution (i.e., 30%, 50%, 70%, and 90% v/v) and, finally, with pure ethanol for 2 min each. The specimens were then dried in 100% hexamethyldisilazane (HMDS; Sigma-Aldrich, USA) for 5 min and later dried in air after the removal of HMDS. After being completely dried, the specimens were affixed on stubs and sputter coated with platinum before observing by FE-SEM. For comparison, the morphology of the cells that had been seeded or cultured on a glass substrate (covered glass slide, 1 mm in diameter; Menzel, Germany) was used as positive control.

Statistics and Data Analysis

All of the quantitative data were presented as mean ± standard deviation. Statistical comparisons were carried out by the one-way analysis of variance (one-way ANOVA) with SPSS 13.0 for

Windows software (SPSS, USA). The statistical significance was considered at P values < 0.05.

RESULTS AND DISCUSSION

Physiochemical of Neat eSF and Surface-Modified eSF Fiber Mats

At 10 wt % Silk/PEO aqueous solutions, the eSF fibers were prepared under different weight ratio of aqueous SF/PEO blends (i.e., 50 : 50 to 90 : 10 weight ratio of SF : PEO) in order to fabricate into electrospun fibers. The electrospinning of these solutions were carried out at EFS of 12–14 kV and 15 cm from the slow-rotating cylindrical drum as a collector under different relative humidity. Figure 1 shows the morphology of eSF/PEO that was obtained by FE-SEM. At 60% RH, a large number of beaded fibers were obtained with the decreasing of PEO concentration (i.e., in the range of 70 : 30 to 90 : 10 weight ratio of SF : PEO), whereas electrospinning below 30% RH results in uniform and bead-free fibers in every concentration. After MeOH treatment and PEO extraction, the obtained fibers at blended PEO concentration lower than 70 : 30 of SF : PEO can be still in the form of fibers. Therefore, the fibers prepared at aqueous 70 : 30 SF/PEO blend (<30% RH) were selected for further experiment, because the higher SF concentration resulted in larger fiber diameters.

Figure 2 shows the morphology and distribution of eSF fibers obtained in each condition. The removal of PEO did not affect the fiber morphology but significantly changed in average fiber diameter at 70 : 30 weight ratio of SF : PEO. The average diameter of as-spun SF/PEO fibers is 407 ± 60 nm. The average fiber diameter increased slightly to 414 ± 73 nm after methanol treatment as a result of α-helix to β-sheet transition while retaining integrity and smoothness on the fiber. However, the average fiber diameter is reduced to 290±46 nm without changing the overall morphology after PEO extraction, where FTIR results showed that no PEO is left in the fibers. The PEO extracted eSF fibers showed an even fiber size distribution which means that PEO solution was homogeneously distributed during the preparation phase. Further surface modification also yielded smooth continuous fibers that were 270 ± 44 nm in diameter.

The FT-IR spectra which is well known to be a sensitive method to confirm the chemical conformation, Figure 3 shows that after MeOH treatment, the strong absorption bands of amide I (stretching) and amide II (N–H deformation and C–N stretching) at 1642 and 1532 cm^{-1} shifted to 1622 and 1512 cm^{-1}, respectively, which indicated the structure conformation from α-helix or random coil to β-sheet conformation transition.[27] Washing of treated the eSF fiber mats at 37°C for 3 days, resulted in extraction of PEO which show the essential absence of distinctive PEO peak at 1109 cm^{-1} (C–O stretching), 963 cm^{-1} (C–H out of plane), and 843 cm^{-1} (C–H out of plane).[19]

After surface modification, the existence of fibronectin on the surface of eSF fibers mat by using EDC/NHS coupling reaction was further evaluated. There was a contributing absorption peak corresponding to the carbonyl (stretching) at 1663 cm^{-1}. Additionally, the absorption of a broad peak in the range of 3000–3600 cm^{-1} corresponding to the N–H stretching of the NH_2 group further confirmed the successful immobilization of the fibronectin on the surface of eSF fiber mats.[31]

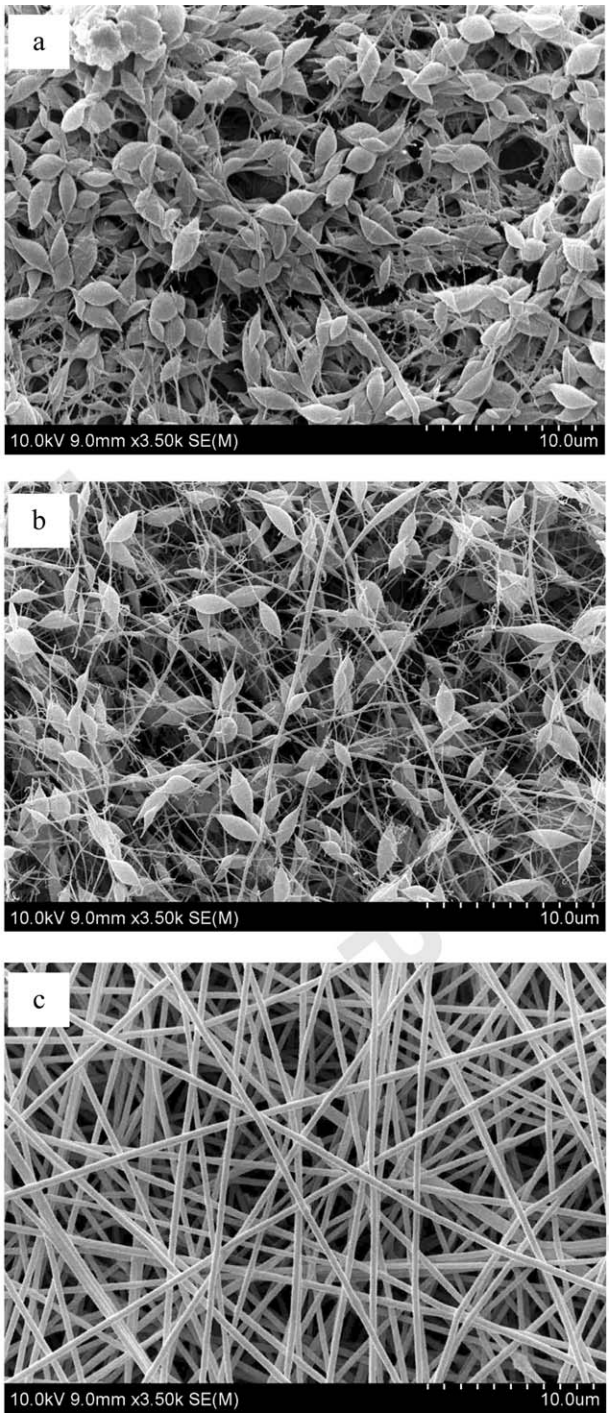

Figure 1. SEM micrographs of eSF/PEO fibers at different humidity: (a) RH ~ 60%, (b) RH ~ 45%, and (c) RH < 30%. Weight ratio of SF/PEO is 70 : 30 in 10%(w/v) of aqueous solution with an applied electric field strength of 14 kV/15 cm.

Surface Elemental Composition

The XPS spectra show the elemental components of neat and surface-modified eSF fibers on the surface. The typical peaks of

Applied Polymer SCIENCE

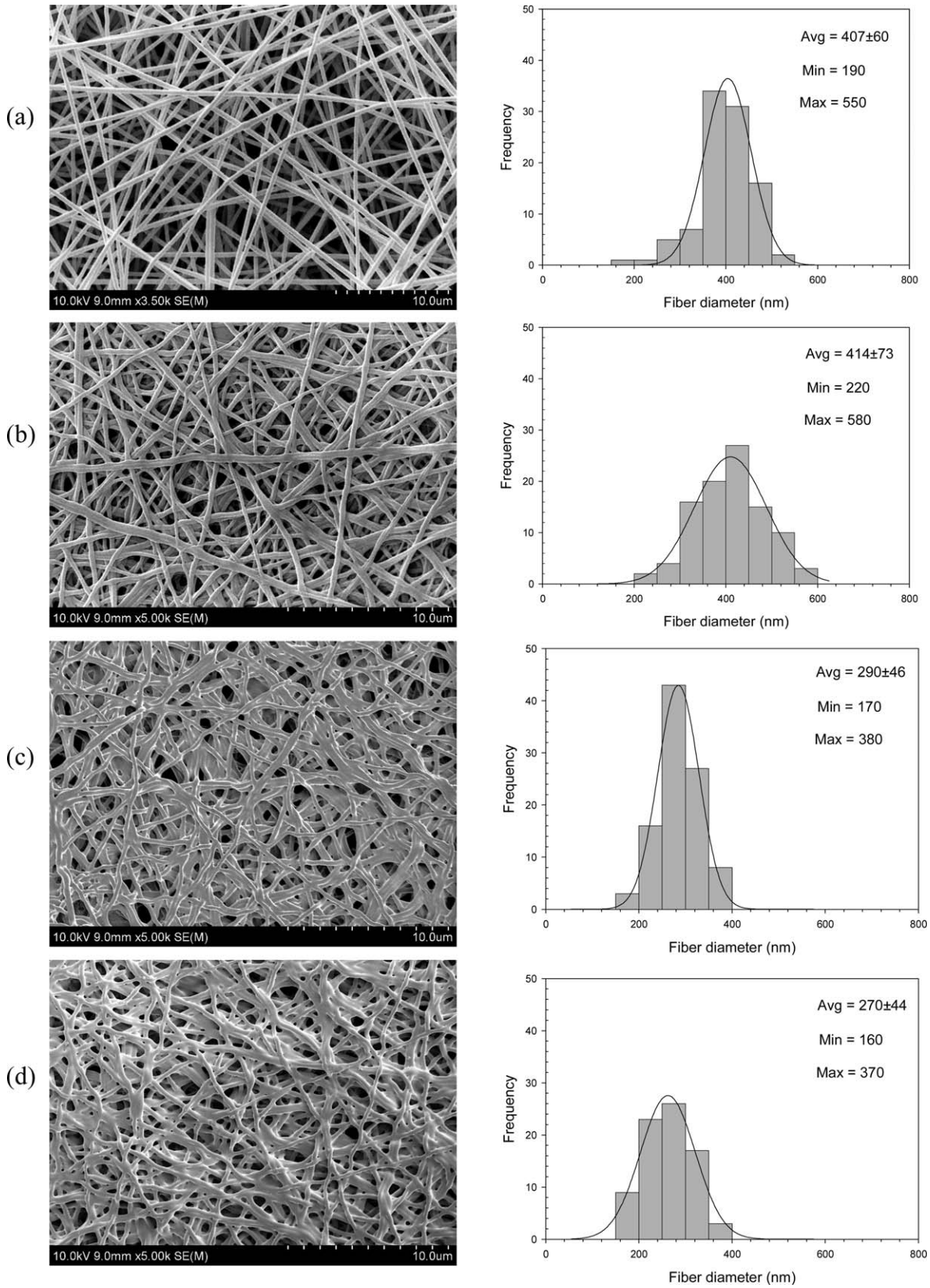

Figure 2. The morphology and fiber diameter at various states of electrospinning of SF nanofibers of: (a) eSF/PEO fibers, (b) MeOH treated SF/PEO fibers, (c) eSF fibers after PEO extraction, and (d) surface-modified eSF fibers. Applied electric field strength was 14 kV/15 cm.

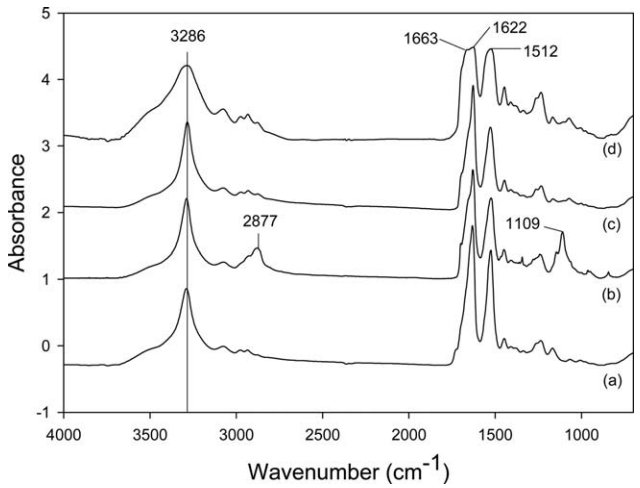

Figure 3. FTIR spectrums of different states SF proteins: (a) SF film, (b) eSF/PEO fiber mat, (c) eSF fiber mat after PEO extraction, and (d) surface-modified eSF fiber mat.

C 1s, N 1s, and O 1s were obviously observed at 284.6 ± 0.2, 398.3 ± 0.2, and 531.0 ± 0.2 eV of binding energy, respectively.[29] The results of elemental concentrations (in at.%), the N/C, O/C ratios and chemical functions (at.%) of surface before and after modification are reported in Table I. In comparison, the carbon (C), nitrogen (N), and oxygen (O) elemental compositions (in at.%) in the eSF fibers surface are 67.4%, 9.5%, and 23.2%, whereas the surface-modified eSF by fibronectin are 63.6%, 16.0%, and 20.4% respectively. The increasing of N/C ratio was obviously observed after modification. Nonetheless, the chemical reaction was also investigated by monitoring the components from curve fitting in C1s photoelectron peaks. Figure 4 shows three components in C 1s peak, which were found in both types of fibers. The components are assigned as: C–(C,H) centered at 285.0 ± 0.2 eV, C–(O,N) centered at 286.5 ± 0.2 eV, and O–C=O centered at 288.1 ± 0.2 eV.[32] According to the coupling reaction, a decrease in percentage of C–(O,N) was found that assigned to the carboxylate functions of the SF protein. Simultaneously, the O–C=O and C–(C,H) was significantly increased that may be originated from side chains of amino acids of the coupling of fibronectin on the fiber surface. The data obtained from O 1s and N 1s were in agreement with the C 1s information.

Water Retention and Dissolution Behavior

To study the potential use of fiber mats that require direct contact with wound exudates, water absorption and dissolution behavior of eSF fiber mats was investigated in PBS buffer solution at physiological temperature of 37°C for 3-day period. Figure 5 shows the difference of water retention capacity and mass remaining of both fiber mats. At initial time period (i.e., 15 min), the water retention of the neat eSF and surface-modified eSF occurred more rapidly when they were immersed in medium with the property value of surface-modified eSF being slightly lower than neat mats, i.e., 123.21% and 77.62%, respectively. A further increase of submersion time resulted in an increase in the water retention of both types of fiber mats to finally become saturated at the equivalent property values after 24 h of submersion of 181.42% and 180.19%, respectively. At the same time, mass remaining of both fiber mats was observed along submersion time. The weight of both types of fibers slightly decreased during their submersion in PBS because of partial disintegration of fiber mat. In comparison, at initial submersion time of 15 min, the dissolution of surface-modified eSF fiber mat was occurring rapidly in which remaining weight was lower than the neat ones. After 3 days of submersion, the weight of neat and surface-modified eSF fiber mats decreased to 93.93% and 91.72%, respectively. It can be obviously observed that surface-modification did not effect to the dissolution behavior of the eSF fibers. The rapid dissolution rate of surface-modified eSF fiber mats may be because of partial disintegration that can be attributed by desorption of fibronectin proteins.

Indirect Cytotoxicity Evaluation

The biocompatibility of Thai SF fiber mat was evaluated on the cytotoxicity of these materials in this study as they were fabricated via electro-spinning process with PEO, known toxic substance, in blending for preparation of SF into the electrospun fiber mats. NHDFs were used as reference in the assessment that had been cultured with extraction medium in comparison with fresh cultured media (i.e., control). The results are shown in Figure 6. Three extraction ratios of the extraction media (i.e., 5, 10, 20 mg/mL) were investigated. Evidently, both the neat and surface-modified eSF fiber mats were nontoxic to the NHDF. The cell viability of NHDF was in the range of 84–120% based on the viability of the cells that had been cultured with fresh cultured medium. Interestingly, the viability of the cells for surface-modified eSF fiber mats was higher than the neat for all extraction ratios. With regards to the surface-

Table I. XPS Surface Chemical Compositions and Elemental Ratio of eSF Fibers Before and After Modification with Fibronectin

	Surface atomic composition (at.%)			Elemental composition ratio		Chemical functions (at.%)				
	C 1s	N 1s	O 1s	N/C	O/C	285.0[a] C—(C,H)	286.5[a] C—(O,N)	288.1[a] O—C=O	533.1[a] C—O	531.9[a] C=O
eSF fibers	67.4	9.5	23.2	0.14	0.34	22.3	31.5	13.7	12.4	10.7
Surface-modified eSF fibers	63.6	16.0	20.4	0.25	0.32	27.6	20.2	15.9	4.2	16.1

[a] Binding energy (eV).

Applied Polymer SCIENCE

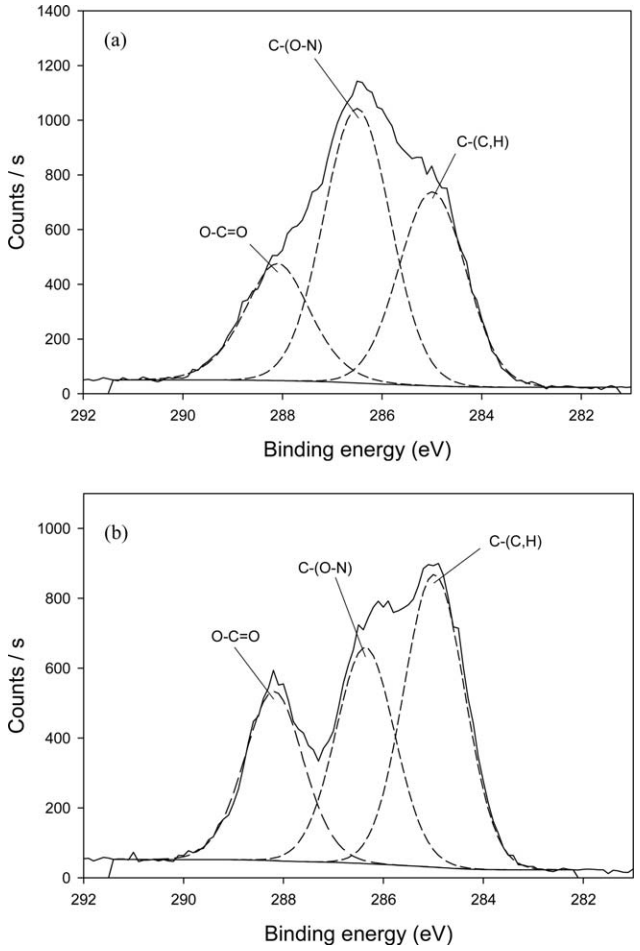

Figure 4. XPS photoelectron peaks of C 1s of: (a) eSF and (b) surface-modified eSF fiber mat. The different chemical compositions obtained from peak fitting are shown.

modified eSF fiber mats, the viability of the cells cultured in the lowest extraction ratio (i.e., 5 mg/mL) from the fiber mats was ~120%, which was significantly greater than that of the extraction medium from the neat one. Based on the results obtained, the extraction medium from both types of fiber mats did not release any harmful substance to the fibroblast. These materials could be further evaluated for their potential on wound healing.

Cell Attachment and Cell Proliferation

Wound healing is a unique biological process which is related to many physiological parameters that automatically occur under normal condition.[2] Since the absence of cytotoxicity, the initial attachment and proliferation might be an important contributing factor for tissue remodeling. Both eSF fiber mats, which mimic a natural ECM, were studied as a supporting cell growth by using human normal fibroblasts which are one of the most abundant cell types in connective tissue that function to maintain tissue homeostasis when tissues are injured.[4] Figure 7 shows the absorbance value signifying the viabilities of the cells that had been cultured on the surfaces of both eSF fiber mat and glass substrate (i.e., control). NHDF were seeded on the surface of these substrates for 2, 4, and 8 h. for the attachment study and 1, 2, and 3 day(s) for proliferation study. For both types of eSF fiber mats, the viability of the attached cells increased monotonically with an increasing of culturing time (Figure 7a). At all culturing time points investigated, the viability of the cells that attached on the surface of both eSF fiber mats was significantly greater than the control, which could be because of biocompatibility of the SF protein and the large surface area of nanofiber construction that is available for cell to attach. The attachment of the NHDF on the eSF fiber mats was further improved with the immobilization of fibronectin on the surface. For the proliferation study (Figure 7b), it was interesting to observe that the surface-modified eSF fiber mats show greater cell viability in any culturing time point, whereas the viability of the NHDF on the neat eSF fiber mat was less than that of the control after they had been cultured on the surface for 2 days. The surface of eSF fibers mats might be considered as rough when the size of pore was much smaller than those of cell that have proliferated priority in 2D direction. However, the cell proliferation can be influenced by the orientation and the biocompatibility of the eSF fibers. The introduction of fibronectin onto the surface of eSF fibers could induce the cells to proliferate inside the porous structure (3D direction) since fibronectin contain the cell-binding domain RGD, which have been known to play a critical role in cell behavior because they regulate gene expression by the signal transduction set by cell adhesion to a functional biomaterial. Moreover, it should be

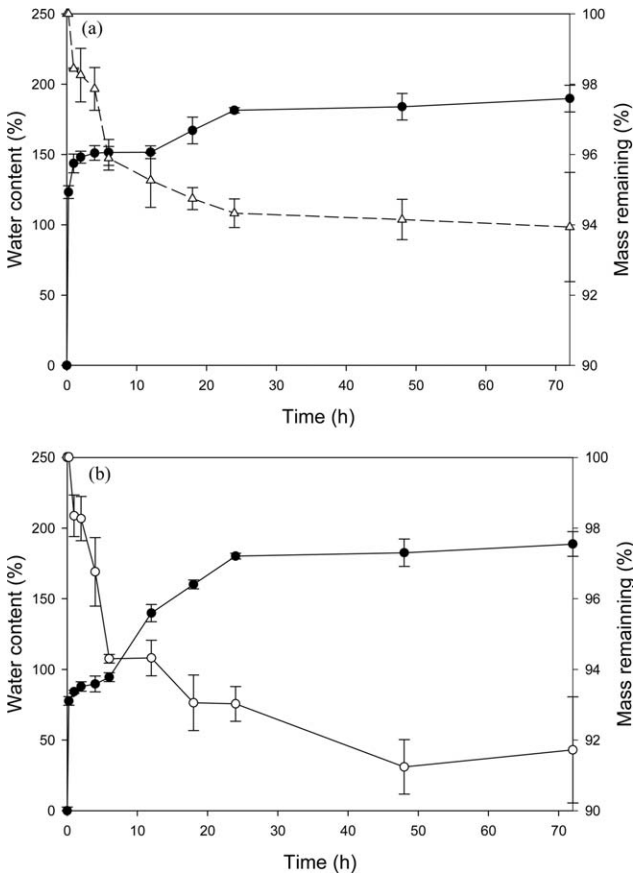

Figure 5. Water retention capacity (●) and dissolution (○) of: (a) eSF and (b) surface-modified eSF fiber mat at various time points in PBS buffer at 37°C.

noted that the large surface area of the surface-modified eSF fiber mats nanofibers play a role on enhanced cell growth and proliferation.

Morphology of Cultured Cells

Tables II and III, respectively, show the representative SEM images of attachment and proliferation activity of NHDF that was cultured on the surface of both types of eSF fibers mat and glass substrate at various culture time. According to Table II, at 2 h after cell seeding, NHDF attachment on both types of eSF fiber mat and the glass substrate started to extend their filopodia, which are thin fiber-like cytoplasmic projections, to create their anchorage on the fiber surfaces. At 4 and 8 h after cell seeding, the cells on both fiber mats and glass substrate further extended their filopodia around the leading egde with strong evident of lemellipodia while those on fibronectin-modified eSF fiber mat were the flattest in shape of migrating cells. The cells on both fibers mats were well extended with direction that might be created by the fibers in comparison to those on glass substrate that were still in round shape. During the proliferation period according to Table III, evidently appeared on fibronectin-modified eSF fibers mat, the cells that had been seeded on all substrates were well expanded in their cytoplasm in the form of thin and long spindle-like shape at 1 day after cell culturing. By further increasing the culturing time to 2 and 3 days, the cells appeared in their typical spindle morphology and spreaded over the surface for all substrate. Interestingly, while the majority of the cells growth on the fibronectin-modified eSF fibers similarly assumed the spindle morphology as the other, the viability of the cells that had been cultured on these fibers surface was always greater than that on others substrate. As previously mentioned, saturation of the viability of

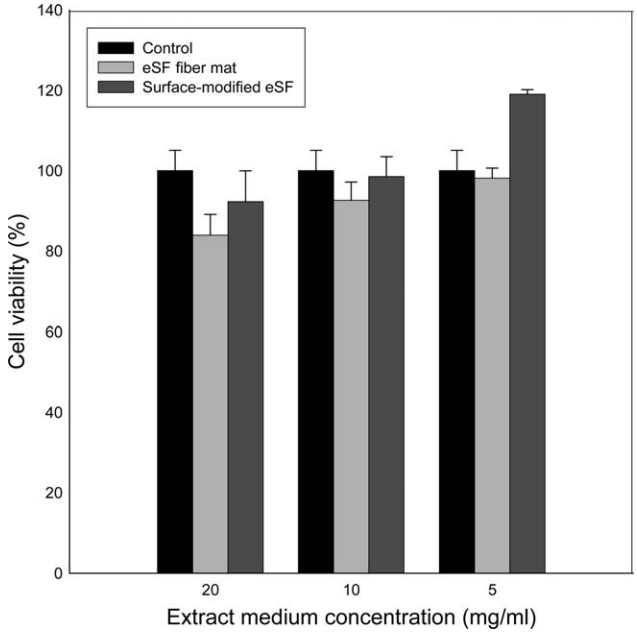

Figure 6. Indirect cytotoxicity evaluation of the neat and modified eSF fiber mat based on the viability of NHDF cultured with various extraction media concentration for 24 h.

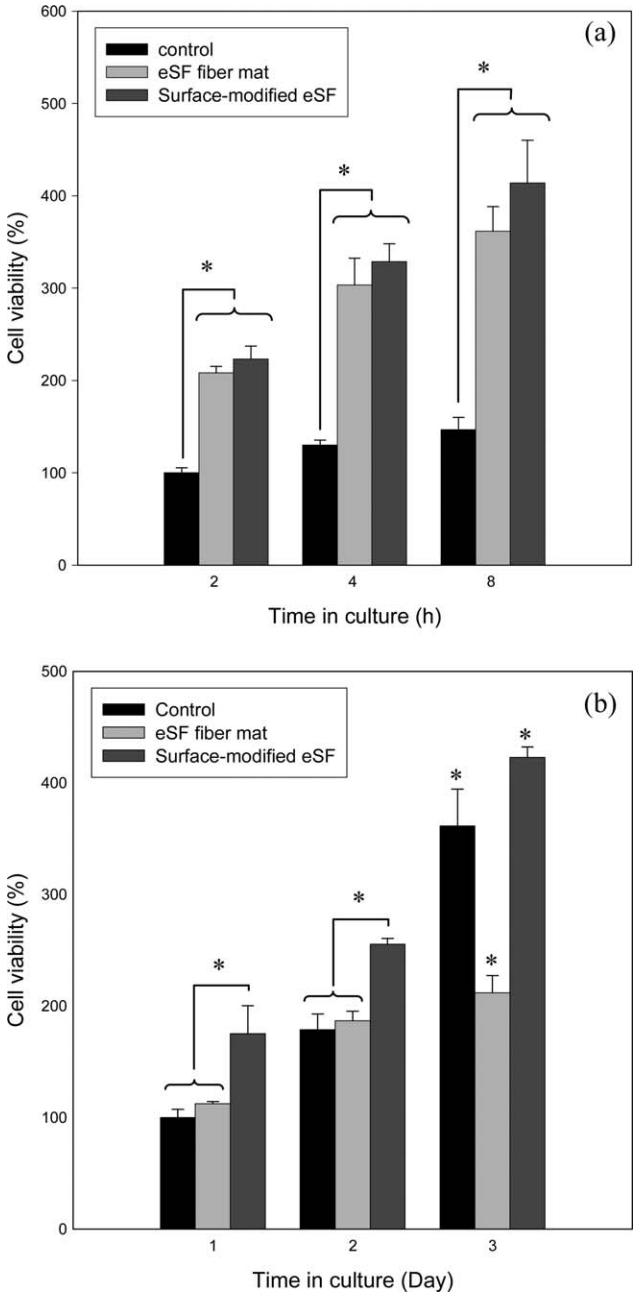

Figure 7. Cell viability of NHDF (a) attachment and (b) proliferation. The NHDF were either seeded or cultured on control, eSF fiber mat, and surface-modified eSF fiber mat as a function of time.

the cells might be because of the migration of the cells onto the hypothetical monolayer construct, even though they were on three-dimensional scaffold. It should be noted that the limitation of the cell morphology study is based on the selection areas of cells, which is a small number of cells imaged. However, the representative SEM images were selected based on the similarity of at least three cell images in each area.

To investigate cell migration behavior, cross-section images of neat and surface-modified eSF fibers were further evaluated as shown in Figure 8. Prior to cell seeding, neat (Figure 8a) and

Table II. SEM Images of Human Dermal fibroblasts (NHDF) Attachment on Glass Slide (i.e., Control), Electrospun Silk Fibroin Fibers (eSF) and Surface-Modified eSF Fibers for 2, 4, and 8 h. (magnification = 500×)

	Type of substrate		
Culturing time	Glass	eSF fibers	Surface-modified eSF fibers
2 h	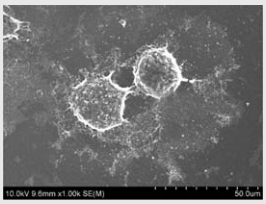	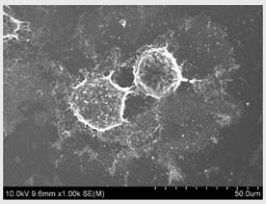	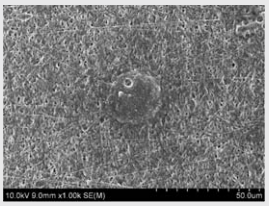
4 h	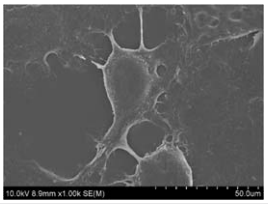	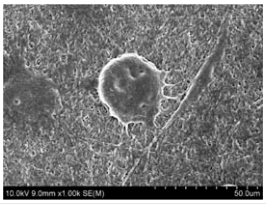	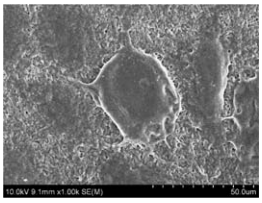
8 h	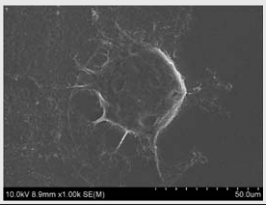		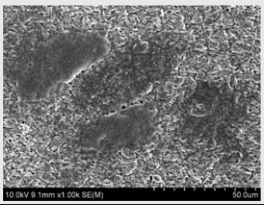

surface-modified eSF fiber mat (Figure 8c) also show the bundle of fiber along the cross-section surface. Interestingly, 3 days after cell seeding, the fiber layer construction of the neat eSF mat was still observed on the cross-section of the eSF fiber mats (Figure 8a), while that of surface-modified eSF fiber mats were filled up with the empty space that could be because of the

Table III. SEM Images of Human Dermal fibroblasts (NHDF) Proliferation Cultured on Glass Slide (i.e., control), Electrospun Silk Fibroin Fibers (eSF) and Surface-Modified eSF Fibers for 1, 2, and 3 d. (magnification = 1000×)

	Type of substrate		
Culturing time	Glass	eSF fibers	Surface-modified eSF fibers
1 d	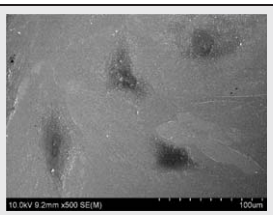	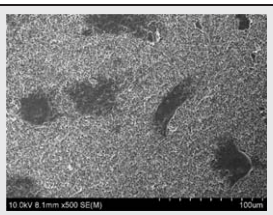	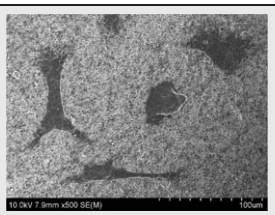
2 d	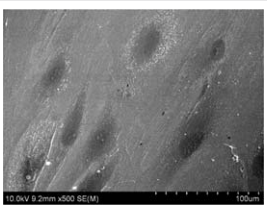	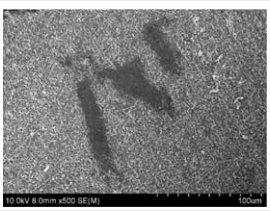	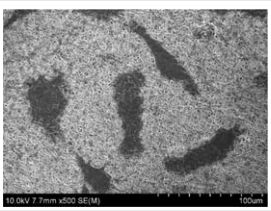
3 d	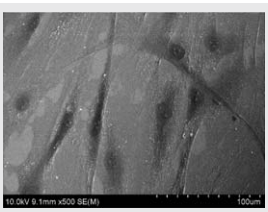	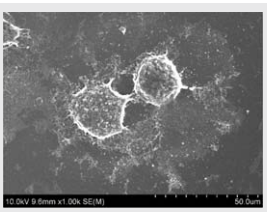	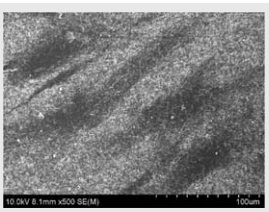

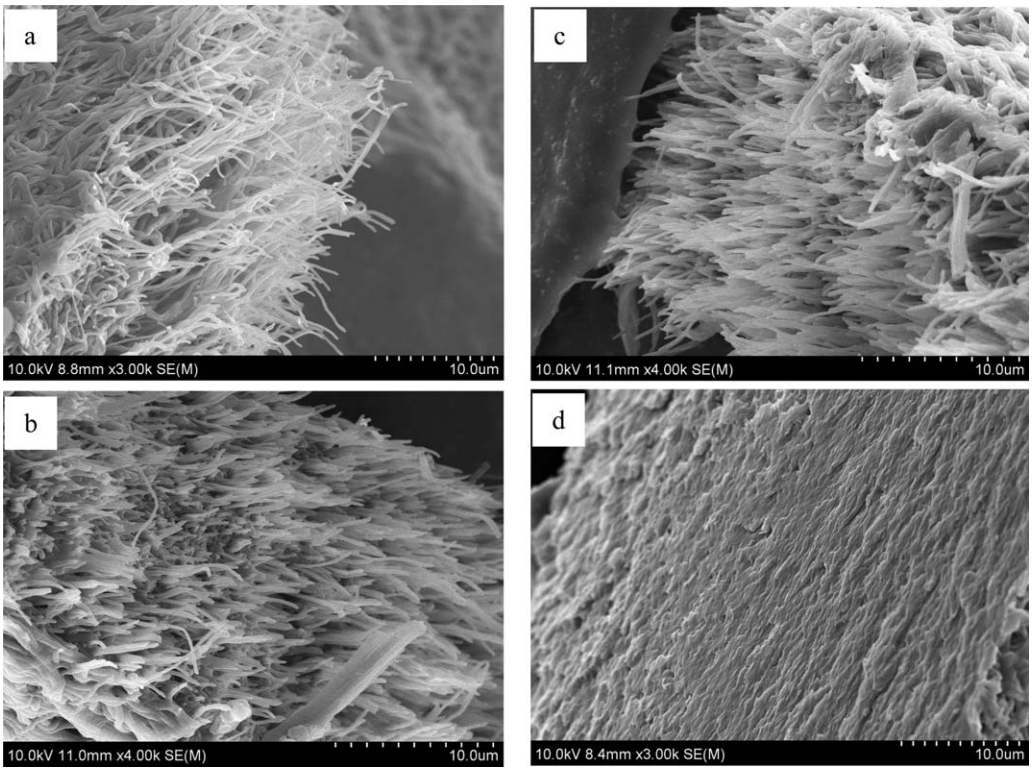

Figure 8. Cross-section images of: (a,b) neat eSF fibers mat and (c,b) surface-modified eSF fibers mat before and after cell culture for 3 days, respectively (magnification = 3000×).

propagation of the cells within the inner layer to form a three-dimensional connective tissue (Figure 8d).

CONCLUSIONS

This study explored a novel biomaterial-scaffold design to achieve the ultra-fine nanofibers with surface modification for bioactive wound dressing. eSF was successfully fabricated from electropinning 70 : 30 weight ratio of SF : PEO, PEO with molecular weight of 600 kDa, in aqueous solution at RH<30%. These fibrous mats had fibers with an average diameter of the individual fibers that were 290 ± 46 nm via PEO extraction, which did not affect the morphology of the fiber mat. Fibronectin was used to immobilize by the carbodiimide chemistry method on the surface of eSF fiber mat. ATR-FTIR data confirmed the existence of the immobilized fibronectin, whereas the XPS spectra indicated the grafting efficiency of the O–C=O and C–(C,H) was significantly increased because of the coupling of fibronectin on the fiber surface. The potential use of neat and surface-modified eSF fiber mats as wound dressing or tissue-remodeling material was assessed with NHDF. Indirect cytotoxic evaluation revealed that both neat and modified eSF fiber mat released no substance that was harmful to the cells. Significantly, the surface-modified eSF fiber mat showed the greatest ability to support the attachment and proliferation of NHDF. Visual observation based on SEM revealed that NHDF cells migrate into the empty space of the fiber mat to form a three dimensional connective tissue. These results demonstrate that eSF mats with surface modification of fibronectin are of great interest for biomedical application especially for accelerated wound healing.

ACKNOWLEDGMENTS

The authors acknowledge partial support received from (a) the National Nanotechnology Center (grant number: BR0108), (b) the National Center of Excellence for Petroleum, Petrochemicals, and Advanced Materials (NCE-PPAM), and (c) the Petroleum and Petrochemical College, Chulalongkorn University, Thailand. J. Chutipakdeevong acknowledges a doctoral scholarship received from the Thailand Graduate Institute of Science and Technology (TGIST) (TG-55-09-51-035D).

REFERENCES

1. Ovington, L. *Clin. Dermatol.* **2007**, *1*, 33.
2. Schreml, S.; Szeimies, R. -M.; Prantl, L.; Landthaler, M.; Babilas, P. *J. Am. Acad. Dermatol.* **2010**, *5*, 866.
3. Zahedi, P.; Rezaeian, I.; Ranaei-Siadat, S.-O.; Jafari, S.-H.; *Supaphol, P. Polym. Adv. Technol.* **2009**, *21*, 77.
4. Li, B.; Wang, J. H. C. *J. Tissue Viabil.* **2011**, *20*, 108.
5. Agarwal, S.; Wendorff, J. H.; Greiner, A. *Polymer* **2008**, *26*, 5603.
6. Alessandrino, A.; Marelli, B.; Arosio, C.; Fare, S.; Tanzi, M. C.; Freddi, G. *Eng. Life Sci.* **2008**, *3*, 219.
7. Altman, G. H.; Diaz, F.; Jakuba, C.; Calabro, T.; Horan, R. L.; Chen, J.; Lu, H.; Richmond, J.; Kaplan, D. L. *Biomaterials* **2003**, *3*, 401.

8. Hardy, J. G.; Scheibel, T. R. *Prog. Polym. Sci.* **2010**, *9*, 1093.
9. Vepari, C.; Kaplan, D. L. *Prog. Polym. Sci.* **2007**, *8-9*, 991.
10. Wadbua, P.; Promdonkoy, B.; Maensiri, S.; Siri, S. *Int. J. Biol. Macromol.* **2010**, *5*, 493.
11. Zhou, C.-Z.; Confalonieri, F.; Medina, N.; Zivanovic, Y.; Esnault, C.; Yang, T.; Jacquet, M.; Janin, J.; Duguet, M.; Perasso, R.; Li, Z.-G. *Nucleic Acids Res.* **2000**, *12*, 2413.
12. Yang, M.; Kawamura, J.; Zhu, Z.; Yamauchi, K.; Asakura, T. *Polymer* **2009**, *1*, 117.
13. Fan, H.; Liu, H.; Toh, S. L.; Goh, J. C. H. *Biomaterials* **2008**, *8*, 1017.
14. Hofmann, S.; Wong Po Foo, C. T.; Rossetti, F.; Textor, M.; Vunjak-Novakovic, G.; Kaplan, D. L.; Merkle, H. P.; Meinel, L. J. *Controlled Release* **2006**, *1–2*, 219.
15. Jin, H. *Biomaterials* **2004**, *6*, 1039.
16. Kim, K.; Jeong, L.; Park, H.; Shin, S.; Park, W.; Lee, S.; Kim, T.; Park, Y.; Seol, Y.; Lee, Y. J. *Biotechnol.* **2005**, *3*, 327.
17. Lee, E.-H.; Kim, J.-Y.; Kweon, H. Y.; Jo, Y.-Y.; Min, S.-K.; Park, Y.-W.; Choi, J.-Y.; Kim, S.-G. *Oral. Surg. Oral. Med. Oral. Pathol. Oral. Radiol. Endod.* **2010**, *5*, e33
18. Meechaisue, C.; Wutticharoenmongkol, P.; Waraput, R.; Huangjing, T.; Ketbumrung, N.; Pavasant, P.; Supaphol, P. *Biomed. Mater.* **2007**, *3*, 181.
19. Meinel, A. J.; Kubow, K. E.; Klotzsch, E.; Garcia-Fuentes, M.; Smith, M. L.; Vogel, V.; Merkle, H. P.; Meinel, L. *Biomaterials* **2009**, *17*, 3058.
20. Meinel, L.; Hofmann, S.; Karageorgiou, V.; Kirker-Head, C.; McCool, J.; Gronowicz, G.; Zichner, L.; Langer, R.; Vunjak-Novakovic, G.; Kaplan, D. L. *Biomaterials* **2005**, *2*, 147.
21. Min, B.-M.; Lee, G.; Kim, S. H.; Nam, Y. S.; Lee, T. S.; Park, W. H. *Biomaterials* **2004**, *7-8*, 1289.
22. Schneider, A.; Wang, X. Y.; Kaplan, D. L.; Garlick, J. A.; Egles, C. *Acta Biomater.* **2009**, *7*, 2570.
23. Wang, Y.; Kim, H.-J.; Vunjak-Novakovic, G.; Kaplan, D. L. *Biomaterials* **2006**, *36*, 6064.
24. Zhang, X.; Baughman, C. B.; Kaplan, D. L. *Biomaterials* **2008**, *14*, 2217.
25. Zhang, X.; Reagan, M. R.; Kaplan, D. L. *Adv. Drug Delivery Rev.* **2009**, *12*, 988.
26. Zarkoob, S.; Eby, R. K.; Reneker, D. H.; Hudson, S. D.; Ertley, D.; Adams, W. W. *Polymer* **2004**, *11*, 3973.
27. Chen, C.; Chuanbao, C.; Xilan, M.; Yin, T.; Hesun, Z. *Polymer* **2006**, *18*, 6322.
28. Li, C.; Vepari, C.; Jin, H.-J.; Kim, H. J.; Kaplan, D. L. *Biomaterials* **2006**, *16*, 3115.
29. Bai, L.; Zhu, L.; Min, S.; Liu, L.; Cai, Y.; Yao, J. *Appl. Surf. Sci.* **2008**, *10*, 2988.
30. Richert, L.; Boulmedais, F.; Lavalle, P.; Mutterer, J.; Ferreux, E.; Decher, G.; Schaaf, P.; Voegel, J.-C.; Picart, C. *Biomacromolecules* **2003**, *2*, 284.
31. Mattanavee, W.; Suwantong, O.; Puthong, S.; Bunaprasert, T.; Hoven, V. P.; Supaphol, P. *ACS Appl. Mater. Interfaces* **2009**, *5*, 1076.
32. Ahimou, F.; Boonaert, C. J. P.; Adriaensen, Y.; Jacques, P.; Thonart, P.; Paquot, M.; Rouxhet, P. G. J. *Colloid Interface Sci.* **2007**, *1*, 49.